Article:

Zhang, K, Zhu, X, Wood, RA et al. (3 more authors) (2018) Oxygenation of the Mesoproterozoic ocean and the evolution of complex eukaryotes. Nature Geoscience, 11 (5). pp. 345-350. ISSN 1752-0894

https://doi.org/10.1038/s41561-018-0111-y

Oxygenation of the Mesoproterozoic ocean and the evolution of complex eukaryotes

Kan Zhang[1,2], Xiangkun Zhu[1*], Rachel A. Wood[3], Yao Shi[1], Zhaofu Gao[1], Simon W. Poulton[2]

[1]MLR Key Laboratory of Isotope Geology, MLR Key Laboratory of Deep-Earth Dynamics, Institute of Geology, Chinese Academy of Geological Sciences, Beijing, 100037, China.

[2]School of Earth and Environment, University of Leeds, Leeds, LS2 9JT, UK.

[3]School of Geosciences, University of Edinburgh, Edinburgh, EH9 3FE, UK.

[*]e-mail: xiangkunzhu@163.com

Abstract

The Mesoproterozoic Era (1,600-1,000 million years ago; Ma) has long been considered a period of relative environmental stasis, with persistently low levels of atmospheric oxygen. There remains much uncertainty, however, over the evolution of ocean chemistry during this time period, which may have been of profound significance for the early evolution of eukaryotic life. Here, we present rare earth element, iron speciation and inorganic carbon isotope data to investigate the redox evolution of the 1,600-1,550 Ma Yanliao Basin, North China Craton. These data confirm that the ocean at the start of the Mesoproterozoic was dominantly anoxic and ferruginous. Significantly, however, we find evidence for a progressive oxygenation event starting at ~1,570 Ma, immediately prior to the occurrence of complex multicellular eukaryotes in shelf areas of the Yanliao Basin. Our study thus demonstrates that oxygenation of the Mesoproterozoic environment was far more dynamic and intense than previously envisaged, and establishes an important link between rising oxygen and the emerging record of diverse, multicellular eukaryotic life in the early Mesoproterozoic.

The earliest definitive evidence for the evolution of eukaryotes occurs in late Paleoproterozoic marine sediments[1,2], but the subsequent Mesoproterozoic has traditionally been perceived as a period of relative evolutionary stasis[2]. However, emerging evidence from several early Mesoproterozoic localities[3,4,5] increasingly supports a relatively high abundance and diversity of eukaryotic organisms by this time. Moreover, decimeter-scale, multicellular fossils have recently been discovered in early Mesoproterozoic (~1,560 Ma) shelf sediments from the Gaoyuzhuang Formation of the Yanliao Basin, North China Craton[6]. Although their precise affinity is unclear, the Gaoyuzhuang fossils most likely represent photosynthetic algae, and provide the strongest evidence yet for the evolution of complex multicellular eukaryotes as early as the Mesoproterozoic[6].

While molecular oxygen is required for eukaryotic synthesis[7], the precise oxygen requirements of early multicellular eukaryotes, including the Gaoyuzhuang fossils, are unclear. This is exacerbated by the fact that recent reconstructions of oxygen levels across the Mesoproterozoic are highly variable, which has reignited the debate over the role of oxygen in early eukaryote evolution[8,9,10,11]. Thus, in addition to providing insight into the affinity of the Gaoyuzhuang fossils, a detailed understanding of the environmental conditions that prevailed in the Yanliao Basin would also inform on the nature of Earth surface oxygenation through the Mesoproterozoic.

Over recent years, understanding of Mesoproterozoic ocean chemistry has converged on a scenario whereby the deep ocean remained predominantly anoxic and iron-rich (ferruginous) beneath oxic surface waters, with widespread euxinic (anoxic and sulphidic) conditions being prevalent along biologically productive continental margins[12,13,14]. Other studies potentially indicate more variability in ocean redox during the Mesoproterozoic, with the suggestion that mid-depth waters may have become more oxygenated by ~1,400 Ma[10,15,16]. However, this possibility of enhanced ocean oxygenation significantly post-dates the occurrence of the Gaoyuzhuang fossils, and whether later Mesoproterozoic ocean oxygenation was widespread remains unclear. Indeed, in surface waters where photosynthetic eukaryotes had potential to thrive, evidence from organic carbon isotopes on the North China Craton suggests a very shallow chemocline from ~1,650-1,300 Ma[17], while rare earth element (REE) data have been interpreted to reflect very low shallow water O_2 concentrations (~0.2 μM and below) throughout the Mesoproterozoic[18].

Here, we present REE, Fe speciation and inorganic carbon isotope data for marine carbonates from the 1,600-1,550 Ma Yanliao Basin, to investigate ocean redox conditions in the basin where the Gaoyuzhuang fossils were discovered. Our data provide a more direct assessment of potential links between the extent of environmental oxygenation and early eukaryote evolution, and suggest that the long-standing paradigm of the Mesoproterozoic as a period of prolonged environmental stasis requires conceptual reconsideration.

Geological setting and samples

The Jixian Section in the Yanliao Basin, 100 km east of Beijing, China, preserves ~9 km thickness of Proterozoic sedimentary rocks deposited atop Archean-Paleoproterozoic crystalline basement (see Supplementary Information). Our samples were collected from the ~1,600-1,550 Ma Gaoyuzhuang Formation of the Jixian Section. The Gaoyuzhuang Formation is divided into four lithological members (Fig. 1), each of which comprises a shallowing-upward cycle consisting mainly of dolostone and limestone deposited in marine environments ranging from the deeper shelf slope to the supratidal/intertidal zone[19,20] (see Fig. 1 and Supplementary Information for full details of the depositional setting). U-Pb dating of zircons from tuff beds in the lower and upper horizons of the Zhangjiayu Member of the Gaoyuzhuang Formation (Fig. 1) gives ages of 1,577 ± 12 Ma[21] and 1,560 ± 5 Ma[22], respectively.

Evaluating ocean redox chemistry

With the exception of Cerium (Ce), REE are strictly trivalent in seawater and exhibit no intrinsic redox chemistry in most natural waters (the reduction of europium (Eu) from Eu(III) to Eu(II) during magmatic, metamorphic or hydrothermal process is an exception[23], but is unlikely to have occurred in our samples). Solution complexation with ligands and surface adsorption to particles are fundamental processes controlling REE cycling in aquatic environments[24]. REE-carbonate ion complexes are the dominant dissolved species in seawater, with a systematic increase in complexation behaviour occurring from the light to heavy REE[25]. Particulate organic matter, and iron and manganese (oxyhydr)oxides, are the dominant carriers of REE, and the light REE (LREE) are preferentially scavenged by these particles compared to heavy REE (HREE)[24].

These processes result in fractionation among REE, resulting in LREE depletion in oxic seawater[24].

Yttrium (Y) and Holmium (Ho) act as a twin pair due to their similar charge and radius. Silicate rocks or clastic sedimentary rocks generally have chondritic Y/Ho values of ~28, implying no apparent fractionation of Y from Ho[26]. By contrast, seawater is generally characterized by super-chondritic Y/Ho ratio (>44), which results from Ho being scavenged faster than Y[27]. The differential behaviour of Cerium (Ce) is particularly useful as a water column redox indicator. Ce exists in either trivalent or tetravalent form, and in oxygenated water, soluble Ce^{3+} tends to adsorb to Fe and/or Mn (oxyhydr)oxide minerals where oxidation to highly insoluble Ce^{4+} is catalysed, resulting in a negative Ce anomaly in the water column[28]. Therefore, compared to ambient oxic seawater, marine particulates generally have higher LREE/HREE ratios, lower Y/Ho ratios, and smaller negative or even positive Ce anomalies[24]. When these particles settle into suboxic/anoxic deeper waters in a stratified ocean, REE become involved in redox-cycling, whereby particulate Mn, Fe and Ce undergo reductive dissolution, releasing scavenged trivalent REE back into solution[29]. This generates higher LREE/HREE ratios, lower Y/Ho ratios, and smaller negative or even positive Ce anomalies in the anoxic water column[30,31]. However, the original seawater REE patterns can be retained in coeval non-skeletal carbonates, thus providing fundamental information on ocean redox conditions[31].

Diagenetic alteration and non-carbonate contamination (e.g., REE in clay minerals) are two factors that require consideration prior to the interpretation of REE data[32]. However, carbonate-REE are generally robust to post-depositional process such as diagenesis or dolomitization[33], and most samples evaluated in our study have experienced little diagenetic recrystallization and only very early dolomitization (based on petrographic features observed under optical microscopy and cathodoluminescence; see Supplementary Information). Although some dolomites from the fourth member of the Gaoyuzhuang Formation show a unimodal, nonplanar texture which may reflect late burial dolomitization, these samples retain typical seawater-like REE patterns (Fig. 1a), suggesting little modification of REE patterns. To address the potential for non-carbonate contamination, we utilized a sequential dissolution method for REE using dilute acetic acid (see Methods), which enables REE in carbonates to be specifically targeted[34]. In addition, no obvious co-variation was observed between Al, Sc, or Th (as indicators of detrital materials) and various REE parameters (e.g., the sum of REE (ΣREE), Y/Ho ratios, the fractionation between LREE and HREE (Pr_n/Er_n), or Ce anomalies (Ce_n/Ce_n^*); see Supplementary Fig. 5). These observations provide strong support for preservation and extraction of primary seawater REE signals[32].

The PAAS-normalized REE patterns of the Gaoyuzhuang Formation carbonates show systematic variability which can be categorized into six groups (Fig. 1a). Carbonates from ~0-650 m, including the Guandi Member, the Sangshu'an Member, and the lower part of the Zhangjiayu Member of the Gaoyuzhuang Formation (Group GYZ-1, GYZ-2, GYZ-3-1), show marine REE patterns that are generally not typical of oxic seawater: middle REE (MREE) enrichment, LREE enrichment or nearly flat REE patterns, near chondritic or slightly higher Y/Ho ratios, and absent (or small) Ce anomalies. Samples from ~650-800 m (Group GYZ-3-2) show variable REE patterns, some of which start to show REE patterns and negative Ce anomalies typical of oxic seawater. Samples from 800 m to the top of the section (Group GYZ-3-3 and GYZ-4) show typical oxic marine REE patterns with negative Ce anomalies ($Ce_n/Ce_n^* = 0.69\text{-}0.92$). These temporal trends in REE patterns record the long-term redox evolution of the Yanliao Basin.

In addition to the REE data, we also utilized Fe speciation as an independent redox indicator. Fe speciation is a well-calibrated technique for identifying anoxia in the water column, and is the only technique that enables ferruginous conditions to be directly distinguished from euxinia[14,35]. Besides application to ancient fine-grained siliciclastic marine sediments, Fe speciation can also be successfully applied to carbonate-rich sediments[31,36,37], providing samples contain sufficient total Fe (Fe_T >0.5 wt%) to produce robust interpretations that are not skewed by the potential for Fe mobilization during late-stage diagenesis or deep burial dolomitization[38]. Hence, we only applied Fe speciation to samples with Fe_T >0.5 wt% (Fig. 1), and in addition, our samples were screened for potential modification of primary signals by deep burial dolomitisation (see Supplementary Information).

Fe speciation defines an Fe pool that is considered highly reactive (Fe_{HR}) towards biological and abiological reduction under anoxic conditions, including carbonate-associated Fe (Fe_{carb}), ferric oxides (Fe_{ox}), magnetite (Fe_{mag}) and pyrite (Fe_{py})[39]. Sediments deposited from anoxic waters commonly have Fe_{HR}/Fe_T >0.38, whereas ratios below 0.22 are generally considered to provide a robust indication of oxic depositional conditions[14]. For samples showing evidence of anoxic deposition (i.e., Fe_{HR}/Fe_T >0.38), ferruginous conditions can be distinguished from euxinia by the extent of pyritization of the Fe_{HR} pool, with Fe_{py}/Fe_{HR} >0.7-0.8 indicating euxinia, and Fe_{py}/Fe_{HR} <0.7 indicating ferruginous conditions[35,40,41].

From 0-800 m in the Gaoyuzhuang Formation, 33 out of 54 samples had Fe_T >0.5 wt% and were deemed suitable for Fe speciation[38], whereas all samples higher in the succession contained <0.5 wt% (Fig. 1c). The samples from 0-800 m show clear evidence for water column anoxia, with high Fe_{HR}/Fe_T >0.38. Furthermore, low Fe_{py}/Fe_{HR} ratios support ferruginous, rather than euxinic, depositional conditions (Fig. 1d). Iron speciation also reveals a significant enrichment in ferric (oxyhydr)oxide minerals in GYZ-3-2 sediments, rather than reduced or mixed valence Fe_{HR} phases, with Fe_{ox} increasing up to 65% of the total Fe_{HR} pool (Fig. 1e) coincident with the first development of REE patterns typical of oxic seawater.

Carbonates were also analyzed for their inorganic carbon isotope ($\delta^{13}C_{carb}$) compositions. Values vary from -2.85‰ to +0.54‰ and are entirely consistent with previous analyses from other parts of the Yanliao Basin (Fig. 2). We interpret these $\delta^{13}C_{carb}$ data to reflect contemporaneous seawater signatures with minimal diagenetic overprint (see Supplementary Information).

Throughout much of the section there is a relatively narrow range in $\delta^{13}C_{carb}$, but a rapid, basin-wide, negative carbon isotope excursion (to values as low as -2.85‰) occurs in the lower part of the Zhangjiayu Member of the Gaoyuzhuang Formation.

Oxygenation of the early Mesoproterozoic ocean

Our REE and Fe speciation data provide strong, independent evidence for anoxic depositional conditions across the lower two members, and the basal part of the Zhangjiayu Member, of the Gaoyuzhuang Formation (GYZ-1, GYZ-2 and GYZ-3-1 in Fig. 1). These samples span a significant range in water depth, from shallow to deeper, distal environments[19,20], suggesting that ferruginous conditions were a prevalent feature of the water column throughout the basin, including in very shallow waters (Fig. 3a). Above this, samples from ~650-800 m (GYZ-3-2 in Fig. 1) have variable REE features, suggesting precipitation around a transitional redox zone. In support of this, Fe speciation data continue to record ferruginous conditions, implying a redox boundary between ferruginous deeper waters and shallower oxic waters. Moreover, an increase in the magnitude of negative Ce anomalies is apparent across this transitional zone (Fig. 1b), which also records a significant increase in the preservation of ferric (oxyhydr)oxide minerals in the sediment (Fig. 1e).

In combination, these observations suggest that our data capture a major transition in water column oxygenation, which resulted in extensive precipitation of Fe (oxyhydr)oxide minerals at the chemocline as ferruginous deeper waters became oxygenated (which is supported by the significant increase in total Fe across this interval; Fig. 1c). Indeed, this transitional redox zone occurs as water depth increases to almost the maximum observed in the succession (Fig. 1), suggesting that a significant rise in surface water oxygen levels resulted in a major deepening of the chemocline, as depicted in Fig. 3b.

REE systematics then support the persistence of well-oxygenated waters throughout the overlying succession, from deep basinal waters, through fluctuating water depths, to very shallow waters. If dissolved oxygen content remained constant as water depth shallowed through time, a change from more negative (in deeper waters) to less negative (in shallower waters) Ce anomalies would naturally occur, due to preferential desorption of light REE relative to Ce(IV) at depth in the water column[42]. Therefore, the relatively stable negative Ce anomalies (and the one sample with a large negative anomaly) as water depth shallows from 800 m to the top of the Gaoyuzhuang Formation (Fig. 1b) imply continued progressive oxygenation of the water column (Fig. 3c). The very low Fe_T content of these samples following large scale drawdown of water column Fe in unit GYZ-3-2 (Fig. 1) is also entirely consistent with an absence of Fe_{HR} (and Fe_{py}) enrichments due to persistent water column oxygenation[38].

Our reconstruction of anoxic ferruginous water column conditions in very shallow waters of the lower Gaoyuzhuang Formation (Fig. 3a) is consistent with previous studies suggesting very low surface water oxygenation in the Mesoproterozoic[17]. However, we also find clear evidence for a progressive oxygenation 'event' beginning at ~1,570 Ma. REE and Fe speciation data are, however, considered to record local to regional water column redox conditions. To place our observations in the more widespread context of the entire Yanliao Basin, we also consider carbon isotope systematics from the Jixian Section and elsewhere in the basin. A prominent negative $\delta^{13}C_{carb}$ excursion, lasting ~1.6 myr (assuming a constant depositional rate), is apparent throughout the Yanliao Basin at ~1,570 Ma (Fig. 2), coincident with the onset of the oxygenation 'event', as recorded independently by our geochemical data. This excursion has previously been attributed to diagenetic alteration[43], but more detailed isotopic studies have suggested that the excursion reflects the development of anoxic bottom waters in deeper basinal environments, which may have resulted in enhanced heterotrophic remineralization under anoxic conditions[19]. However, these previous studies lacked the environmental context afforded by our redox evaluation of the water column, which suggests that, by contrast, the excursion is linked to the development of oxic, rather than anoxic, conditions.

Based on our data, we consider two potential mechanisms to explain the negative $\delta^{13}C_{carb}$ excursion. The first mechanism would require a widespread decline in organic carbon burial, but this is inconsistent with total organic carbon (TOC) data, which shows an increase from <0.1 wt% below the excursion to ~0.5 wt% during the excursion (Supplementary Fig. 7). Instead, we suggest that the negative $\delta^{13}C_{carb}$ excursion is directly related to widespread oxygenation in the basin, and likely reflects the oxidation of a $\delta^{13}C$ depleted pool of dissolved organic carbon and/or methane at the redoxcline. The $\delta^{13}C_{carb}$ record of early Mesoproterozoic successions in the Yanliao Basin also shows a gentle long-term increase to more positive values above the negative isotope excursion (Fig. 2; ref 44), which is also consistent with the progressive longer-term increase in oxygenation indicated by our REE data. This would be consistent with the emerging evidence for possible deeper water oxygenation recorded in marine sediments from the ~1,400 Ma Kaltasy Formation, Russia[16], and in the ~1,400-1,320 Ma Xiamaling Formation, North China[10,15]. These observations suggest that our data may capture the onset of a major, global rise in Mesoproterozoic Earth surface oxygenation, which contrasts with the persistent low-oxygen condition often advocated for this time period[8,9,17,18].

Implications for eukaryote evolution

The complex eukaryotes of the Gaoyuzhuang Formation (Fig. 1) are found in the Zhangjiayu Member[6], shortly after the onset of the oxygenation 'event' recorded by our geochemical data. In addition, the Gaoyuzhuang fossils are found near storm wave base on the shelf (Fig. 3b)[6], suggesting that rising oxygen levels and a concomitant deepening of the oxycline created the environmental stability required for their evolution. This reinforces the role of oxygen as an evolutionary driver in the Mesoproterozoic, and provides support for the suggestion that these complex eukaryotes were likely involved in aerobic respiration and photosynthesis[6]. While

Gaoyuzhuang-type fossils have not yet been discovered elsewhere, several other early Mesoproterozoic successions, including the Ruyang Group (~1,750-1,400 Ma) in the southwestern margin of the North China Craton[3], the Kotuikan Formation (~1,500 Ma) on the northern Siberia Platform[5], and the Roper Group (~1,500 Ma) in northern Australia[4], have been reported to preserve a relatively high abundance and diversity of eukaryotic organisms, in contrast to older strata. This suggests that chemical and biological evolution during the Mesoproterozoic were likely intrinsically linked, and far from static, on a global scale.

In summary, the early Mesoproterozoic Yanliao Basin records an important step-change in Earth's oxygenation history, which was most likely linked to atmospheric oxygenation. The emerging evidence from the North China Craton and elsewhere[10,15,16] suggests that the progressive oxygenation 'event' recorded by our data may have been of global significance, with major implications for eukaryote evolution. While further detailed study of other successions is required to evaluate spatial and temporal constraints on early Mesoproterozoic oxygenation, our data build upon emerging evidence from the fossil record, to suggest that environmental change was likely considerably more dynamic than previously recognised during the far from 'boring' Mesoproterozoic Era.

References

1. Rasmussen, B., Fletcher, I. R., Brocks, J. J. & Kilburn, M. R. Reassessing the first appearance of eukaryotes and cyanobacteria. *Nature* **455,** 1101-1104 (2008).
2. Knoll, A. H., Javaux, E. J., Hewitt, D. & Cohen, P. Eukaryotic organisms in Proterozoic oceans. *Philos Trans R Soc Lond B Biol Sci* **361,** 1023-1038 (2006).
3. Agić, H., Moczydłowska, M. & Yin, L. Diversity of organic-walled microfossils from the early Mesoproterozoic Ruyang Group, North China Craton - a window into the early

eukaryote evolution. *Precambrian Research* **297,** 101-130 (2017).

4. Javaux, E. J., Knoll, A. H. & Walter, M. R. Morphological and ecological complexity in early eukaryotic ecosystems. *Nature* **412,** 66-69 (2001).
5. Vorob'eva, N. G., Sergeev, V. N. & Petrov, P. Y. Kotuikan Formation assemblage: A diverse organic-walled microbiota in the Mesoproterozoic Anabar succession, northern Siberia. *Precambrian Research* **256,** 201-222 (2015).
6. Zhu, S. et al. Decimetre-scale multicellular eukaryotes from the 1.56-billion-year-old Gaoyuzhuang Formation in North China. *Nat Commun* **7,** 11500 (2016).
7. Summons, R. E., Bradley, A. S., Jahnke, L. L. & Waldbauer, J. R. Steroids, triterpenoids and molecular oxygen. *Philos Trans R Soc Lond B Biol Sci* **361,** 951-968 (2006).
8. Lyons, T. W., Reinhard, C. T. & Planavsky, N. J. The rise of oxygen in Earth's early ocean and atmosphere. *Nature* **506,** 307-315 (2014).
9. Planavsky, N. J. et al. Low Mid-Proterozoic atmospheric oxygen levels and the delayed rise of Animals. *Science* **346,** 635-638 (2014).
10. Zhang, S. et al. Sufficient oxygen for animal respiration 1,400 million years ago. *Proc Natl Acad Sci* **113,** 1731-1736 (2016).
11. Daines, S. J., Mills, B. J. & Lenton, T. M. Atmospheric oxygen regulation at low Proterozoic levels by incomplete oxidative weathering of sedimentary organic carbon. *Nat Commun* **8,** 14379 (2017).
12. Poulton, S. W., Fralick, P. W. & Canfield, D. E. Spatial variability in oceanic redox structure 1.8 billion years ago. *Nature Geoscience* **3,** 486-490 (2010).
13. Planavsky, N. J. et al. Widespread iron-rich conditions in the mid-Proterozoic ocean. *Nature* **477,** 448-451 (2011).
14. Poulton, S. W. & Canfield, D. E. Ferruginous Conditions: A Dominant Feature of the Ocean through Earth's History. *Elements* **7,** 107-112 (2011).

15. Wang, X. et al. Oxygen, climate and the chemical evolution of a 1400 million year old tropical marine setting. *American Journal of Science* **317,** 861-900 (2017).

16. Sperling, E. A. et al. Redox heterogeneity of subsurface waters in the Mesoproterozoic ocean. *Geobiology* **12,** 373-386 (2014).

17. Luo, G. et al. Shallow stratification prevailed for ~1700 to ~1300 Ma ocean: Evidence from organic carbon isotopes in the North China Craton. *Earth and Planetary Science Letters* **400,** 219-232 (2014).

18. Tang, D., Shi, X., Wang, X. & Jiang, G. Extremely low oxygen concentration in mid-Proterozoic shallow seawaters. *Precambrian Research* **276,** 145-157 (2016).

19. Guo, H. et al. Sulfur isotope composition of carbonate-associated sulfate from the Mesoproterozoic Jixian Group, North China: Implications for the marine sulfur cycle. *Precambrian Research* **266,** 319-336 (2015).

20. Mei, M. Preliminary study on sequence-stratigraphic position and origin for Molar-tooth structure of the Gaoyuzhuang Formation of Mesoproterozoic at Jixian section in Tianjin. *Journal of Palaeogeography* **7,** 437-447 (2005).

21. Tian, H. et al. Zircon LA-MC-ICPMS U-Pb dating of tuff from Mesoproterozoic Gaoyuzhuang Formation in Jixian Country of North China and its geological significance. *Acta Geoscientica Sinica* **36,** 647-658 (2015).

22. Li, H. et al. Further constraints on the new subdivision of the Mesoproterozoic stratigraphy in the northern North China Craton. *Acta Petrologica Sinica* **26,** 2131-2140 (2010).

23. Michard, A., Albarède, F., Michard, G., Minster, J. F. & Charlou, J. L. Rare-earth elements and uranium in high-temperature solutions from East Pacific Rise hydrothermal vent field (13 ºN). *Nature* **303,** 795-797 (1983).

24. Sholkovitz, E. R., Landing, W. M. & Lewis, B. L. Ocean particle chemistry: The fractionation of rare earth elements between suspended particles and seawater. *Geochimica et*

Cosmochimica Acta **58,** 1567-1579 (1994).

25. Cantrell, K. J. & Byrne, R. H. Rare earth element complexation by carbonate and oxalate ions. *Geochimica et Cosmochimica Acta* **51,** 597-605 (1987).
26. Bau, M. Controls on the fractionation of isovalent trace elements in magmatic and aqueous systems: evidence from Y/Ho, Zr/Hf, and lanthanide tetrad effect. *Contrib Mineral Petrol* **123,** 323-333 (1996).
27. Nozaki, Y., Zhang, J. & Amakawa, H. The fractionation between Y and Ho in marine environment. *Earth and Planetary Science Letters* **148,** 329-340 (1997).
28. Bau, M. & Koschinsky, A. Oxidative scavenging of cerium on hydrous Fe oxides: Evidence from the distribution of rare earth elements and yttrium between Fe oxides and Mn oxides in hydrogenetic ferromanganese crusts. *Geochemical Journal* **43,** 37-47 (2009).
29. German, C. R., Holliday, B. P. & Elderfield, H. Redox cycling of rare earth elements in the suboxic zone of the Black Sea. *Geochimica et Cosmochimica Acta* **55,** 3553-3558 (1991).
30. Bau, M., Moller, P. & Dulski, P. Yttrium and lanthanides in eastern Mediterranean seawater and their fractionation during redox-cycling. *Marine Chemistry* **56,** 123-131 (1997).
31. Tostevin, R. et al. Low-oxygen waters limited habitable space for early animals. *Nat Commun* **7,** 12818 (2016).
32. Nothdurft, L. D., Webb, G. E. & Kamber, B. S. Rare earth element geochemistry of Late Devonian reefal carbonates, Canning Basin, Western Australia: confirmation of a seawater REE proxy in ancient limestones. *Geochimica et Cosmochimica Acta* **68,** 263-283 (2004).
33. Banner, J. L., Hanson, G. N. & Meyers, W. J. Rare earth elements and Nd isotopic variations in regionally extensive dolomites from the Burlington-Keokuk Formation (Mississippian): Implications for REE mobility during carbonate diagenesis. *Journal of Sedimentary Petrology* **58,** 415-432 (1988).
34. Zhang, K., Zhu, X. & Yan, B. A refined dissolution method for rare earth element studies of

bulk carbonate rocks. *Chemical Geology* **412,** 82-91 (2015).

35. Poulton, S. W., Frallck, P. W. & Canfield, D. E. The transition to a sulphidic ocean ~1.84 billion years ago. *Nature* **431,** 173-177 (2004).

36. Clarkson, M. O. et al. Dynamic anoxic ferruginous conditions during the end-Permian mass extinction and recovery. *Nat Commun* **7,** 12236 (2016).

37. Wood, R. A. et al. Dynamic redox conditions control late Ediacaran metazoan ecosystems in the Nama Group, Namibia. *Precambrian Research* **261,** 252-271 (2015).

38. Clarkson, M. O., Poulton, S. W., Guilbaud, R. & Wood, R. A. Assessing the utility of Fe/Al and Fe-speciation to record water column redox conditions in carbonate-rich sediments. *Chemical Geology* **382,** 111-122 (2014).

39. Poulton, S. W. & Canfield, D. E. Development of a sequential extraction procedure for iron: implications for iron partitioning in continentally derived particulates. *Chemical Geology* **214,** 209-221 (2005).

40. Poulton, S. W. & Raiswell, R. The low-temperature geochemical cycle of iron: From continental fluxes to marine sediment deposition. *American Journal of Science* **302,** 774-805 (2002).

41. Raiswell, R. & Canfield, D. E. Sources of iron for pyrite formation in marine sediments. *American Journal of Science* **298,** 219-245 (1998).

42. Ling, H. et al. Cerium anomaly variations in Ediacaran–earliest Cambrian carbonates from the Yangtze Gorges area, South China: Implications for oxygenation of coeval shallow seawater. *Precambrian Research* **225,** 110-127 (2013).

43. Li, R., Chen, J., Zang, S. & Chen, Z. Secular variations in carbon isotopic compositions of carbonates from Proterozoic successions in the Ming Tombs Section of the North China Platform. *Journal of Asian Earth Sciences* **22,** 329-341 (2003).

44. Guo, H. et al. Isotopic composition of organic and inorganic carbon from the Mesoproterozoic

Jixian Group, North China: Implications for biological and oceanic evolution. *Precambrian Research* **224,** 169-183 (2013).

Acknowledgements

This work was supported by NSFC Grant 41430104 and CAGS Research Fund YYWF201603 to X.K.Z., a China Scholarship Council award to K.Z. and a China Geological Survey Grant DD20160120-04 to Bin Yan. S.W.P. acknowledges support from a Royal Society Wolfson Research Merit Award. We thank Linzhi Gao and Pengju Liu for field guidance, and Fuqiang Shi, Chao Tang, Xi Peng, Chenxu Pan, Nina Zhao, Chuang Bao, Zilong Zhou and Yueling Guo for field work assistance. We acknowledge Feipeng Xu and Miao Lv for assistance in elemental analysis, Yijun Xiong for help with Fe speciation experiments, Yanan Shen, Kefan Chen and Wei Huang for carbon isotope analyses, and Fred Bowyer for assistance with cathodoluminescence. We also express our thanks to Jin Li, Da Li, Yuan He, Jianxiong Ma, Xinjie Zou and Kun Du for logistical support.

Author contributions

X.K.Z. designed the project. X.K.Z., K.Z., Y.S., Z.F.G. did fieldwork and collected samples. K.Z. carried out elemental and Fe speciation analyses. R.A.W. provided expertise in the evaluation of carbonate diagenesis. X.K.Z., K.Z. and S.W.P. interpreted the data, and K.Z., S.W.P. and X.K.Z. wrote the paper, with additional input from all co-authors.

Competing financial interests

The authors declare no competing financial interests.

Figure captions

Figure 1: Summary of sedimentary facies (SF) and geochemical signals for carbonates from

the Gaoyuzhuang Formation, Jixian Section. (a) PAAS-normalized REE patterns categorized into six groups. (b) Cerium anomaly profile (see Supplementary Information for calculation details). (c) Total Fe (Fe_T) profile (analytical precision is within the size of the symbols). (d) Fe speciation results (see text for details). (e) Fe_{ox}/Fe_{HR} profile. Sea level reached its highest around the middle Gaoyuzhuang Formation[19,20].

Figure 2: Compilation of inorganic carbon isotope ($\delta^{13}C_{carb}$) data for the Gaoyuzhuang Formation across the Yanliao Basin. Jixian Section (this study); Pingquan Section (ref 44); Ming Tombs Section (ref 43) (see Supplementary Fig. 1a for sample locations). Analytical precision is within the size of the symbols.

Figure 3: Cartoon depicting the redox evolution of the early Mesoproterozoic Yanliao Sea. Three stages are depicted, including the relative position of carbonates analyzed for the present study: (a) In the earliest Mesoproterozoic, seawater was anoxic and ferruginous with a very shallow chemocline; (b) The chemocline deepened, likely to below storm wave base, around the middle of Gaoyuzhuang Formation, in response to the onset of oxygenation. The increase in shallow water oxygenation coincides with the presence of decimeter-scale, complex multicellular eukaryotes; (c) The extent of ocean oxygenation continued to increase with time.

Methods

Rare Earth Elements

The chemical dissolution of REE was carried out in a class 100 ultra-clean laboratory. The dissolution method applied has been reported elsewhere[34]. Briefly, the technique initially dissolves 30-40% of total carbonate, followed by a subsequent extraction of the next 30-40% of total carbonate using dilute acetic acid (0.5 mol/L), which was sampled for REE and considered to best represent that of the carbonate source water. Elemental analysis, including REE, Th, Sc, Ca, Mg and Al in carbonate leachates, was conducted via ICP-MS and ICP-OES, with replicate extractions giving a RSD of less than 3% for these elements.

Fe-speciation and total Fe

Fe-speciation extraction was performed using standard sequential extraction protocols[39]. Iron in carbonate minerals (Fe_{carb}) was extracted with a sodium acetate solution at pH 4.5, for 48 h at 50ºC; Iron (oxyhydr)oxide minerals (Fe_{ox}) were then extracted with a sodium dithionite solution at pH 4.8 for 2 h at room temperature; Finally, magnetite Fe (Fe_{mag}) was extracted with an ammonium oxalate solution for 6 h at room temperature. All Fe concentrations were measured via atomic absorption spectrometry (AAS) with replicate extractions giving a RSD of <5% for all phases. Total iron (Fe_T) were determined by one of two methods: 1. X-Ray Fluorescence; 2. A HNO_3-HF-$HClO_4$ digest on ashed samples (overnight at 550°C) followed by AAS analysis. Pyrite iron (Fe_{py}) was calculated on the basis of the weight percentage of sulphur extracted during chromous chloride distillation[45], with a RSD of <5%.

Inorganic carbon isotopes

To determine $\delta^{13}C_{carb}$, carbonate powders of ~150 µg were first reacted with anhydrous phosphoric acid at 70°C to extract CO_2 using a KEIL IV carbonate device. The produced CO_2 was then purified stepwise and ultimately introduced into a Finnigan MAT 253 mass spectrometer. Carbon isotope determinations were performed using a dual-inlet mode against an in-house standard reference gas in the mass spectrometer. All values are reported as $\delta^{13}C_{carb}$ relative to the Vienna Peedee Belemnite (VPDB) standard. The precision is better than 0.06‰ based on replicate analyses of the Chinese national standard GBW04416 ($\delta^{13}C$ = 1.61 ± 0.03‰).

Data availability

The authors declare that the data supporting the findings of this study are available within the article and its supplementary information files.

References in Methods

45. Canfield, D. E., Raiswell, R., Westrich, J. T., Reaves, C. M. & Berner, R. A. The use of chromium reduction in the analysis of reduced inorganic sulfur in sediments and shales. *Chemical Geology* **54,** 149-155 (1986).

Correspondence and requests for materials should be addressed to Xiangkun Zhu (xiangkunzhu@163.com).

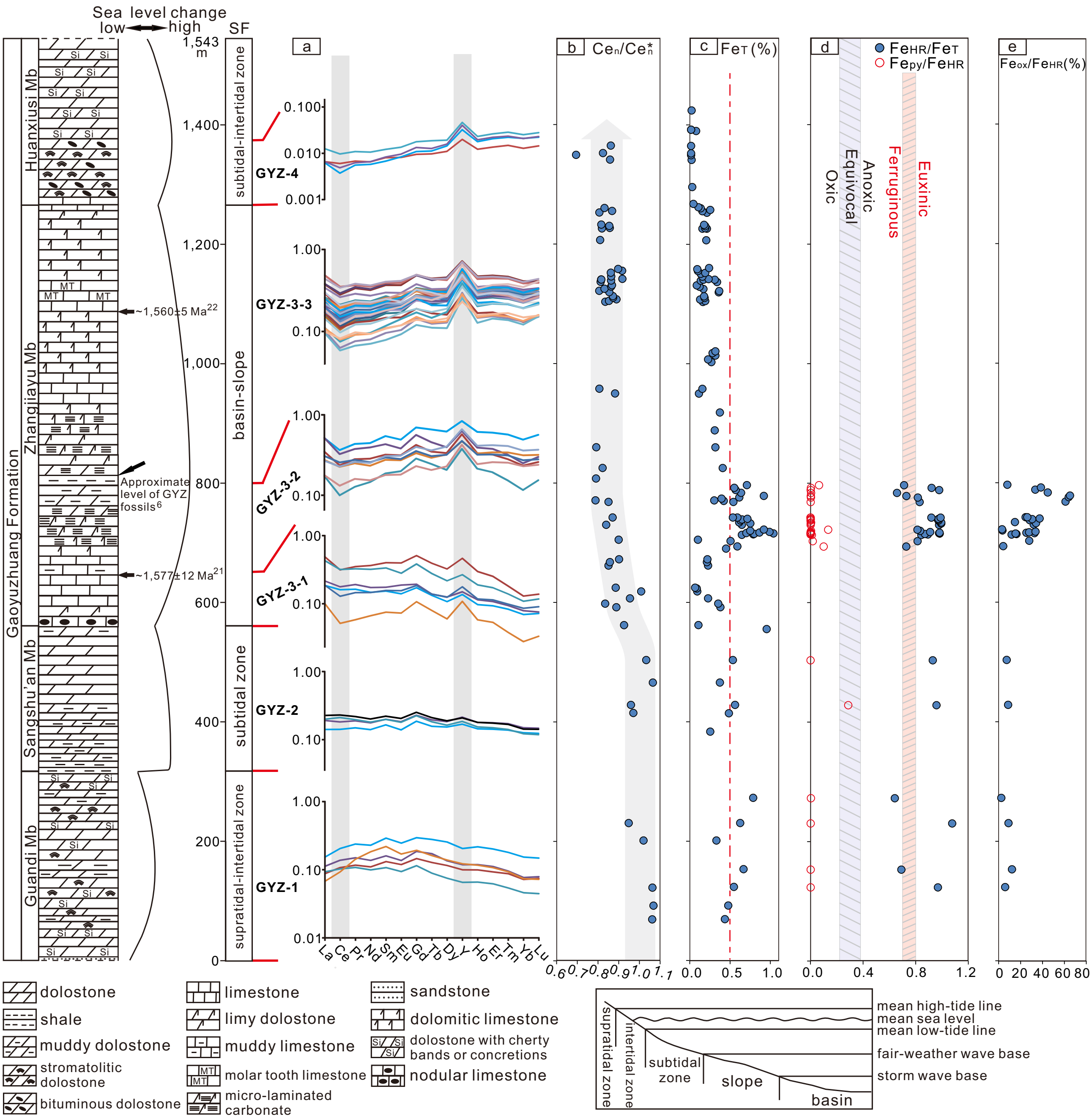

Sea level change
low high
SF
1,543 m
Gaoyuzhuang Formation
Huanxiusi Mb
Zhangjiayu Mb
Sangshu'an Mb
Guandi Mb
~1,560±5 Ma22
Approximate level of GYZ fossils6
~1,577±12 Ma21
subtidal-intertidal zone
basin-slope
subtidal zone
supratidal-intertidal zone
GYZ-4
GYZ-3-3
GYZ-3-2
GYZ-3-1
GYZ-2
GYZ-1
a
b Cen/Ce*n
c FeT (%)
d FeHR/FeT
FePy/FeHR
Oxic
Equivocal
Anoxic
Ferruginous
Euxinic
e Feox/FeHR(%)
La Ce Pr Nd Sm Eu Gd Tb Dy Ho Er Tm Yb Lu
dolostone
shale
muddy dolostone
stromatolitic dolostone
bituminous dolostone
limestone
limy dolostone
muddy limestone
molar tooth limestone
micro-laminated carbonate
sandstone
dolomitic limestone
dolostone with cherty bands or concretions
nodular limestone
mean high-tide line
mean sea level
mean low-tide line
fair-weather wave base
storm wave base
supratidal zone
intertidal zone
subtidal zone
slope
basin

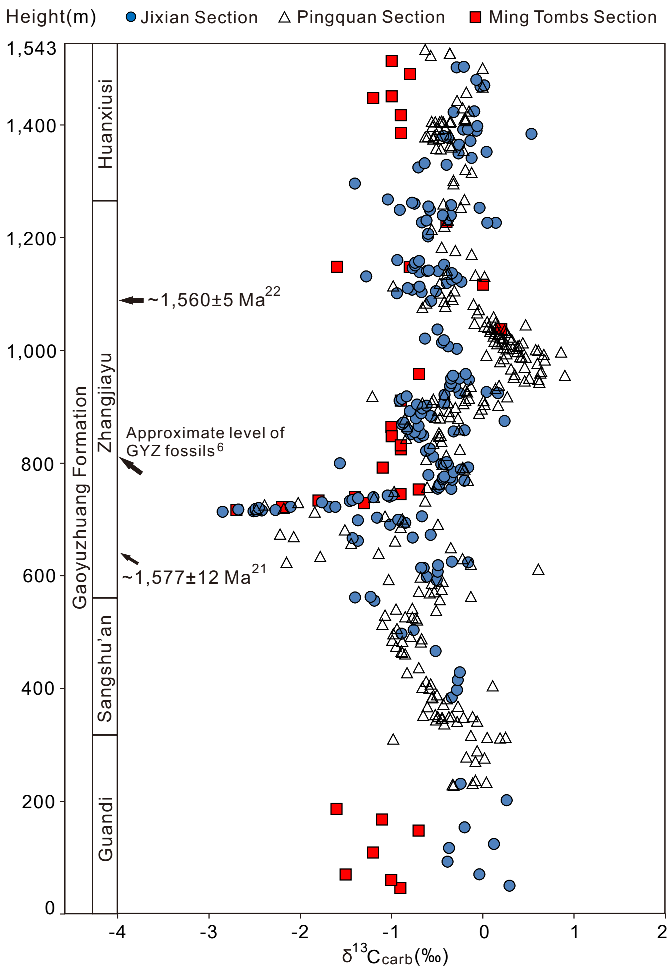
Height(m)
Jixian Section
Pingquan Section
Ming Tombs Section
1,543
1,400
1,200
1,000
800
600
400
200
0
Gaoyuzhuang Formation
Huanxiusi
Zhangjiayu
Sangshu'an
Guandi
~1,560±5 Ma22
Approximate level of GYZ fossils6
~1,577±12 Ma21
-4
-3
-2
-1
0
1
2
δ13Ccarb(‰)

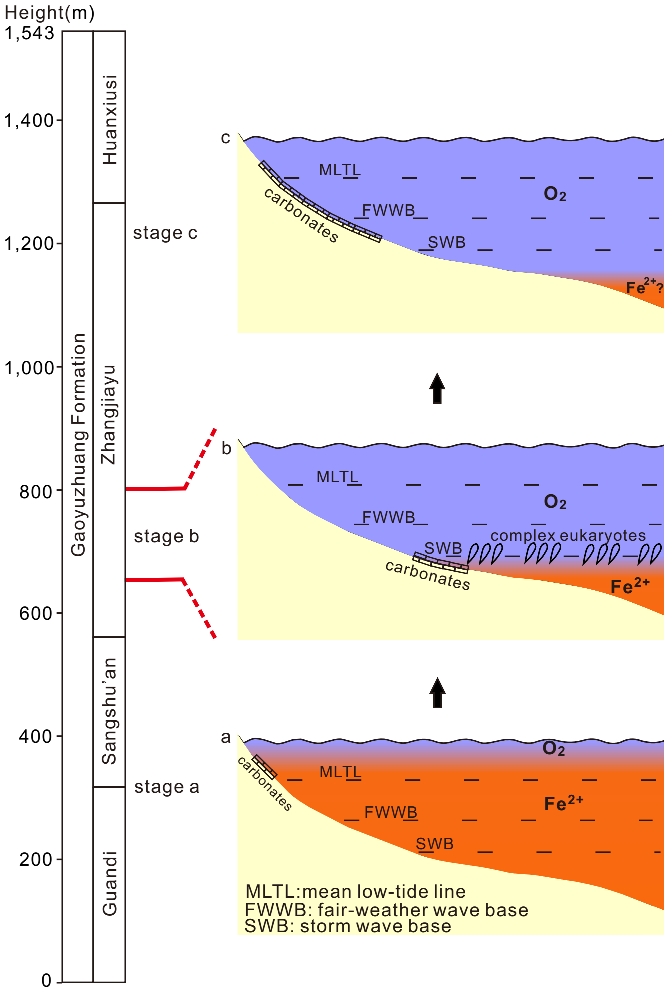

Height(m)
1,543
1,400
1,200
1,000
800
600
400
200
0
Gaoyuzhuang Formation
Huanxiusi
Zhangjiayu
Sangshu'an
Guandi
stage c
stage b
stage a
c
MLTL
FWWB
SWB
carbonates
O2
Fe2+?
b
MLTL
FWWB
SWB
complex eukaryotes
carbonates
O2
Fe2+
a
O2
MLTL
FWWB
SWB
carbonates
Fe2+
MLTL:mean low-tide line
FWWB: fair-weather wave base
SWB: storm wave base